Available online at www.sciencedirect.com
ScienceDirect
Dyes and Pigments 77 (2008) 24–30
DYES and PIGMENTS
www.elsevier.com/locate/dyepig

Decolorization of C.I. Reactive Red 2 in O_3, Fenton-like and O_3/Fenton-like hybrid systems

Chung-Hsin Wu*

Department of Environmental Engineering, Da-Yeh University, 112, Shan-Jiau Road, Da-Tsuen, Chang-Hua 515, Taiwan, ROC

Received 26 December 2006; received in revised form 24 February 2007; accepted 2 March 2007
Available online 12 March 2007

Abstract

The decolorization of C.I. Reactive Red 2 using ozone-related, Fenton-like-related and ozone/Fenton-like hybrid systems was studied. The UV, H_2O_2, UV/Fe^{3+} and H_2O_2/Fe^{3+} systems did not achieve significant decolorization at pH 7; decolorization rates followed the order: pH 10 > pH 7 > pH 4 in the O_3 and UV/O_3 systems and followed the opposite order in the case of the UV/H_2O_2 system. Decolorization rate constants were consistent with pseudo-first-order kinetics. In the O_3 system, decolorization rate declined as dye concentration increased. The decolorization rate constants at pH 7·followed the order UV/O_3/H_2O_2/Fe^{3+} (5.78 h^{-1}) > UV/O_3/H_2O_2 (5.33 h^{-1}) > UV/H_2O_2/Fe^{3+} (4.59 h^{-1}) > UV/H_2O_2 (4.08 h^{-1}) > UV/O_3 (2.91 h^{-1}) = O_3 (2.91 h^{-1}) ≥ UV/O_3/Fe^{3+} (2.90 h^{-1}) > O_3/Fe^{3+} (2.42 h^{-1}) > O_3/H_2O_2/Fe^{3+} (2.03 h^{-1}) > O_3/H_2O_2 (1.42 h^{-1}).
© 2007 Elsevier Ltd. All rights reserved.

Keywords: Advanced oxidation processes; Decolorization; C.I. Reactive Red 2; UV; O_3; Fenton-like

1. Introduction

Azo dyes are by far the largest of all classes of dyes. As the wastewater from textile dyeing typically contains high concentrations of colorants, effective decolorization methods are urgently required. Although numerous physical/chemical schemes, including coagulation, flocculation, adsorption and membrane filtration, have been used to decolorize textile effluents, these techniques suffer disadvantages of sludge generation, adsorbent regeneration and membrane fouling.

Advanced oxidation processes (AOPs) are alternative methods for decolorizing and reducing recalcitrant wastewater loads from the textile dyeing industry. Among the AOPs, treatment with ozone [1–5] or Fenton-type [4–6] processes have yielded very good results. The Fenton-type process combines an iron compound with hydrogen peroxide to produce hydroxyl radicals. Hydrogen peroxide [7,8], OH^- [3], UV light [3,9] and reduced transition metals [1,7,10,11] can activate the decomposition of ozone to hydroxyl radicals. The effects of dye concentration [3,12], ozone dosage [12,13], pH [1,3,12,14], presence or absence of UV [3,9] and UV intensity [9] in ozone-related systems have been evaluated. The general mechanism involves Fenton reagent that utilizes Fe^{2+} (Fenton) or Fe^{3+} (Fenton-like) ions as catalysts to decompose hydrogen peroxide. Ultraviolet irradiation (photo-Fenton and photo-Fenton-like reactions) [15,16] promotes degradation of organic compounds in Fenton and Fenton-like reactions. Several studies have investigated the effects of iron salt dosage [16–19], H_2O_2 dosage [6,16–19], the nature of the iron salt [6,17], the presence or absence of UV [16,17,20] and UV intensity [16] in Fenton-type processes.

Various researchers have explored synergic effects in the decolorization of dyes using hybrid systems, including Fe^0/H_2O_2 [21], O_3/H_2O_2 [7,8,21,22], O_3/Fe^{2+} [23,24], UV/O_3/H_2O_2 [7,22,25], O_3/H_2O_2/Fe^{2+} [7], UV/O_3/Fe^{2+} [11,23,24], UV/O_3/Fe^{3+} [10], UV/TiO_2/O_3 [2,22], UV/TiO_2/H_2O_2 [20], UV/O_3/H_2O_2/Fe^{3+} [22], UV/O_3/Fe^{2+}/Cu^{2+} [11,24], UV/O_3/H_2O_2/Fe^{2+} [7] and UV/O_3/TiO_2/SnO_2 [3]. Several studies have analyzed the factors that influence dye decolorization in H_2O_2- and ozone-related individual systems. Most hybrid H_2O_2-related processes, when used under acidic conditions, achieved a higher decolorization efficiency than that obtained under neutral or alkaline conditions; conversely, hybrid ozone-related processes

* Fax: +886 5 5334958.
E-mail address: chunghsinwu@yahoo.com.tw

0143-7208/$ - see front matter © 2007 Elsevier Ltd. All rights reserved.
doi:10.1016/j.dyepig.2007.03.002

were preferred under alkaline conditions. When H_2O_2- and ozone-related systems were utilized for pre-treating and/or post-treating biological wastewater, the pH must be adjusted twice, firstly to an acidic/alkaline pH for the H_2O_2-/ozone-related systems and, subsequently, adjustment to neutral pH. Thus, a system with high decolorization efficiency under neutral pH is economically attractive. Notably, Fe^{3+} has been assessed in relatively few hybrid H_2O_2-/ozone-related systems; in addition, no study has investigated hybrid H_2O_2-/ozone-related systems at neutral pH.

This work concerns the effect of Fe^{3+} on hybrid H_2O_2-/ozone-related systems on the decolorization of C.I. Reactive Red 2 (RR2) at neutral pH and, notably, to compare the decolorization efficiencies of O_3, O_3/H_2O_2, O_3/Fe^{3+}, $O_3/H_2O_2/Fe^{3+}$, UV/H_2O_2, $UV/H_2O_2/Fe^{3+}$, UV/O_3, $UV/O_3/Fe^{3+}$, $UV/O_3/H_2O_2$ and $UV/O_3/H_2O_2/Fe^{3+}$ systems at neutral pH. The effects of pH in the O_3, UV/H_2O_2 and UV/O_3 systems and the effect of dye concentration in the O_3 systems were also determined.

2. Materials and methods

2.1. Materials

The dye ($C_{19}H_{10}Cl_2N_6Na_2O_7S_2$, 615 g/mol and λ_{max} 538 nm) was obtained from Aldrich. Ferric sulfate ($Fe_2(SO_4)_3$), utilized as the source of Fe^{3+}, was of analytical grade and was purchased from Merck, as was hydrogen peroxide solution (H_2O_2, 30% w/w). pH was controlled using HNO_3 and NaOH via an automatic titrator. All reagents were employed without further treatment; deionized and doubly distilled water was used. In the ozone-related systems, a 137 mm long dielectric barrier discharge (DBD) reactor [3] was utilized to produce ozone. A stainless steel wire (diameter, 5.0 mm) was suspended as an inner electrode along the axis of a Pyrex-glass tube (internal diameter, 20.0 mm). Glass pellets (diameter, 5 mm) were used as packing material and were placed in the plasma region between the two electrodes. The reactor consumed 8 W in pure oxygen at a flow rate of 500 mL/min; the concentration of ozone was fixed at 2060 ppm (in gas) [3].

2.2. Decolorization experiments

The decolorization of RR2 at pH 7 in UV, H_2O_2, UV/Fe^{3+} and H_2O_2/Fe^{3+} systems were determined as background experiments. The dye concentration was 40 ppm in all experiments, except in those that determined the effects of dye concentration in the O_3 system. Decolorization was performed in a 3 L hollow cylindrical glass reactor. Inside the inner quartz tube was an 8 W, 254 nm UV-lamp (Philips) as irradiation source (emission wavelength 230–320 nm). The concentration of Fe^{3+} was 25 ppm; H_2O_2 doses of 500, 1000, 3000, 5000 and 10,000 ppm were used to determine the optimum H_2O_2 dosage. In ozone-related systems, ozone was pumped into the reactor at a flow rate of 500 mL/min while in the non-ozone systems, air was input at 500 mL/min into the reactor to maintain the same experimental conditions. All systems were stirred continuously at 300 rpm. A 15 mL aliquot was withdrawn from the photoreactor at pre-specified intervals from which suspended solids were removed by centrifugation at 5000 rpm for 10 min, followed by filtration through a 0.22 μm filter (Millipore). Decolorization of RR2 was measured using a spectrophotometer (HACH DR/4000U) at 538 nm. Decolorization efficiency was determined from the difference in dye concentrations before and after the experiment.

3. Results and discussion

3.1. Background experiments

When the decolorization efficiency of UV, H_2O_2, UV/Fe^{3+} and H_2O_2/Fe^{3+} systems was determined at pH 7, no significant decolorization (Fig. 1) was achieved. Thus, the oxidizing power of neither UV nor H_2O_2 was adequate to decolorize the dye. In the UV/Fe^{3+} system, the reaction is expressed as Eq. (1) [17,26]

$$Fe^{3+} + H_2O + h\nu \rightarrow Fe^{2+} + H^+ + OH\bullet \quad k = 3.3 \times 10^{-6}\ M^{-1}\ s^{-1} \tag{1}$$

However, OH• may be scavenged by Fe^{2+} according to Eq. (2).

$$Fe^{2+} + OH\bullet \rightarrow Fe^{3+} + OH^- \quad k = 3.2 \times 10^{8}\ M^{-1}\ s^{-1} \tag{2}$$

Since the rate constant in Eq. (1) is considerably lower than that in Eq. (2) [17], the decolorization efficiency of the UV/Fe^{3+} system is negligible, a finding similar to that obtained by Muruganandham and Swaminathan [27] for the UV/Fe^{2+} system.

The typical mechanism of the Fenton reaction involves several cyclical reactions. Based on Eqs. (3)–(8), Fe^{2+} and H_2O_2 are formed in their original state at the end of the cyclical reactions [17,22,26]. When a Fenton-like reagent is applied, the reaction sequence begins with Eq. (4).

$$Fe^{2+} + H_2O_2 \rightarrow Fe^{3+} + OH^- + OH\bullet \quad k = 76\ M^{-1}\ s^{-1} \tag{3}$$

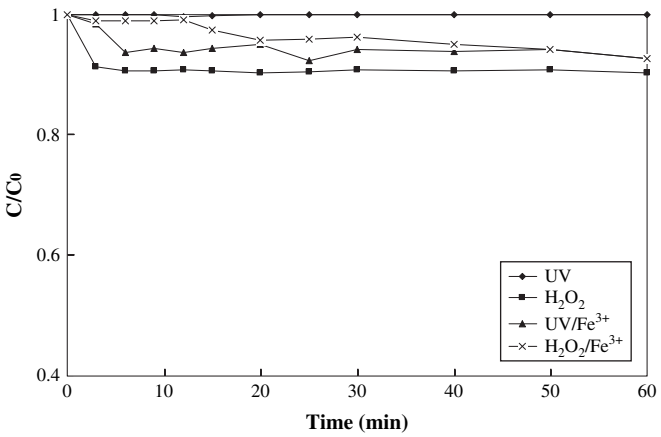

Fig. 1. Decolorization efficiency of UV, H_2O_2, UV/Fe^{3+} and H_2O_2/Fe^{3+} systems (RR2 = 40 ppm, H_2O_2 = 1000 ppm, Fe^{3+} = 25 ppm, pH = 7 and T = 25 °C).

$$Fe^{3+} + H_2O_2 \rightarrow Fe^{2+} + H^+ + HO_2\bullet \quad k = 0.02\ M^{-1}\ s^{-1} \tag{4}$$

$$Fe^{2+} + HO_2\bullet \rightarrow Fe^{3+} + HO_2^- \quad k = 1.2 \times 10^6\ M^{-1}\ s^{-1} \tag{5}$$

$$Fe^{3+} + HO_2\bullet \rightarrow Fe^{2+} + H^+ + O_2 \quad k = 3.1 \times 10^5\ M^{-1}\ s^{-1} \tag{6}$$

$$OH\bullet + H_2O_2 \rightarrow HO_2\bullet + H_2O \quad k = 4.5 \times 10^7\ M^{-1}\ s^{-1} \tag{7}$$

$$2OH\bullet \rightarrow H_2O_2 \quad k = 5.3 \times 10^9\ M^{-1}\ s^{-1} \tag{8}$$

In the H_2O_2/Fe^{3+} system, hydroperoxyl and hydroxyl radicals are generated by Fe^{3+} and Fe^{2+}, according to Eqs. (4) and (3), respectively. However, Fe^{2+} and H_2O_2 scavenge hydroxyl radicals, according to Eqs. (2) and (7), and Fe^{2+} and Fe^{3+} scavenge hydroperoxyl radicals, according to Eqs. (5) and (6), respectively. The negligible decolorization of the H_2O_2/Fe^{3+} system is attributable to the following characteristics:

(i) radical generation rates were lower than consumption rates, as described in Eqs. (2)–(8) [17];
(ii) the Fe^{3+} dosage was low, consequently few radicals were produced.

Since $Fe_2(SO_4)_3$ was utilized as the Fe^{3+} source, the dissociated sulfate may further scavenge hydroxyl radicals, rendering decolorization negligible [28]. Attention must be paid to the molar Fe^{3+}:H_2O_2 ratio to prevent undesired radical scavenging reactions (Eqs. (2) and (5)–(7)) in the presence of excess Fe^{3+} or H_2O_2.

Fig. 2 shows the background UV–vis spectra of H_2O_2, O_3, Fe^{3+} and H_2O_2/Fe^{3+} in solution. The experimental results indicated that H_2O_2 and O_3 in solution are absorbed at wavelengths <310 and <245 nm, and Fe^{3+} and H_2O_2/Fe^{3+} were absorbed at <400 nm. Absorbance intensities at <260 nm followed the order: $H_2O_2/Fe^{3+} > H_2O_2 > Fe^{3+}$, implying that favorable photolysis/photocatalytic conditions can produce radicals. Furthermore, the order of the absorbance intensities follows that of radical production. Hoffmann et al. [29] demonstrated that direct H_2O_2 or O_3 photolysis requires photons with a wavelength <310 nm and that H_2O_2/Fe^{3+} absorbs photons of wavelength up to 550 nm [30]. These experimental results are similar to those obtained in other studies [29,30].

3.2. Decolorization efficiency of H_2O_2 systems

Fig. 3 shows the effect of H_2O_2 dosage at pH 7 in the UV/H_2O_2 system with 500, 1000, 3000, 5000 and 10,000 ppm of H_2O_2 added. Although H_2O_2 did not decolorize RR2, it markedly increased the decolorization efficiency when combined with UV irradiation. Eq. (9) describes the reaction of the UV/H_2O_2 system.

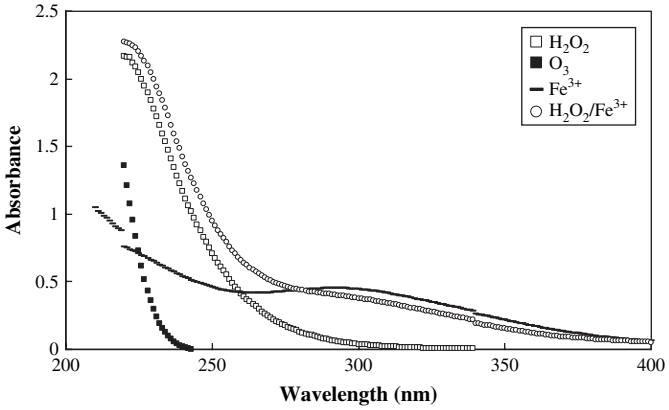

Fig. 2. Background UV–vis spectra of H_2O_2, O_3, Fe^{3+} and H_2O_2/Fe^{3+} in solution (H_2O_2 = 1000 ppm, ozone flow rate = 500 mL/min, Fe^{3+} = 25 ppm, and T = 25 °C).

$$H_2O_2 + h\nu \rightarrow 2OH \tag{9}$$

The degradation rate of organic compounds increases with H_2O_2 concentration up to a threshold; as the H_2O_2 concentration increases further, degradation efficiency declines as H_2O_2 scavenges hydroxyl radicals when present at a high concentration [16,17,19,21], thereby generating hydroperoxyl radicals which have lower oxidation capacity than hydroxyl radicals (Eq. (7)). Additionally, the recombination of hydroxyl radicals

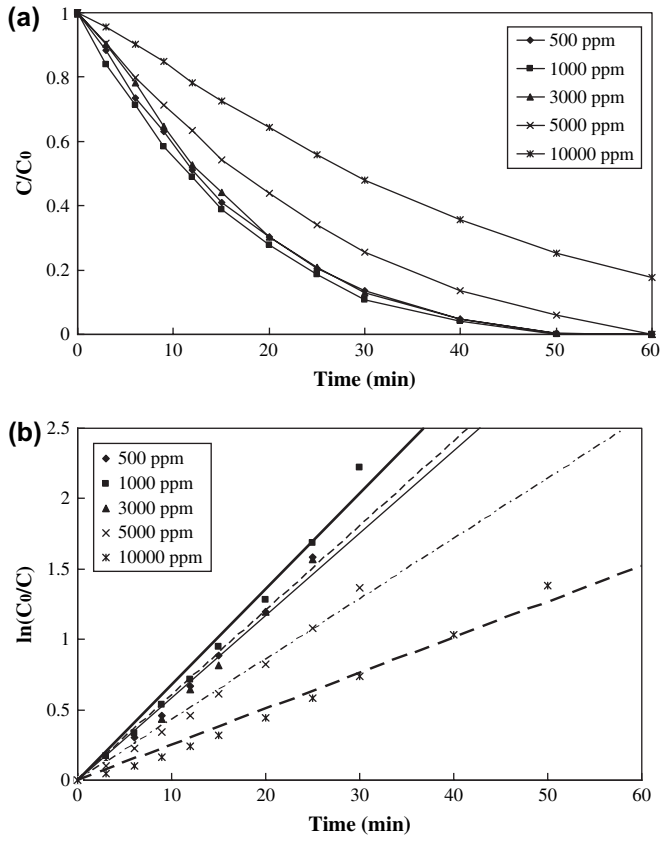

Fig. 3. Effects of H_2O_2 dosage in UV/H_2O_2 system on (a) decolorization efficiency and (b) linear regression of pseudo-first-order reaction kinetics (RR2 = 40 ppm, pH = 7 and T = 25 °C).

also reduces decolorization efficiency (Eq. (8)). Decolorization efficiency increased as the H_2O_2 concentration increased from 500 to 1000 ppm in the UV/H_2O_2 system; however, at concentrations >1000 ppm, no further improvement occurred (Fig. 3(a)). Plotting $\ln(C_0/C)$ as a function of time yielded the decolorization rate constant (k) (Fig. 3(b)). The k values for photocatalytic systems exhibit pseudo-first-order kinetics; numerous studies have indicated that dye decolorization rates can be approximated using pseudo-first-order kinetics [3,18,22,23]. The k values obtained at 500, 1000, 3000, 5000 and 10,000 ppm H_2O_2 in UV/H_2O_2 systems were 3.61, 4.08, 3.51, 2.57 and 1.52 h^{-1}, respectively, and the corresponding correlation coefficients were 0.989, 0.985, 0.979, 0.991 and 0.982, respectively. The hydrogen peroxide:catalyst ratios ranged from 10:1 to 40:1, this being typically recommended as optimal for Fenton processes [31,32]. Based on an appropriate hydrogen peroxide dosage of 1000 ppm and to prevent the generation of a large quantity of sludge, the Fe^{3+} dosage was set at 25 ppm in all experiments in which Fe^{3+} was used.

pH influences the generation of hydroxyl radicals and, therefore, decolorization efficiency. Fig. 4 shows the effect of pH in the UV/H_2O_2 system from which it is evident that UV/H_2O_2 system completely decolorized RR2 after 50 min at pHs of 4 and 7. The decolorization rate constant of the UV/H_2O_2 system followed the order: pH 4 (4.96 h^{-1}) > pH 7 (4.08 h^{-1}) > pH 10 (1.99 h^{-1}) (Table 1), perhaps due to auto-decomposition of H_2O_2 to oxygen and water under alkaline conditions. Buxton et al. [33] demonstrated that the oxidation potential of hydroxyl radicals declines as pH increases. Hence, the decolorization rate constant was lowest at pH 10.

3.3. Decolorization efficiency of the ozone systems

Ozone reacts with dyes either by electrophilic attack or indirectly by radical chain reaction, depending on pH. Fig. 5 shows the effect of pH in the O_3 and UV/O_3 systems. The k values for the UV/O_3 system exceeded those of O_3 and the k values of the O_3 and UV/O_3 systems followed the order: pH 10 > pH 7 > pH 4 (Table 1). Ozone oxidizes organic compounds via two possible degradation routes:

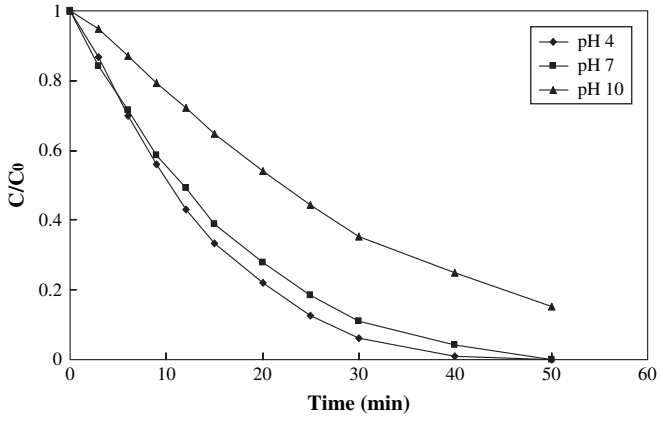

Fig. 4. Effects of pH on the decolorization efficiency in UV/H_2O_2 system (RR2 = 40 ppm, H_2O_2 = 1000 ppm and T = 25 °C).

Table 1
Pseudo-first-order reaction rate constants and correlation coefficients of various systems (RR2 = 40 ppm, H_2O_2 = 1000 ppm and Fe^{3+} = 25 ppm)

Systems	k (h^{-1})	R^2
Non-UV systems		
O_3 (pH 4)	1.67 [1.75]	0.983 [0.989]
O_3 (pH 7)	2.91 [4.19]	0.976 [0.991]
O_3 (pH 10)	5.74 [7.36]	0.996 [0.997]
O_3/H_2O_2 (pH 7)	1.42	0.994
O_3/Fe^{3+} (pH 7)	2.42	0.948
$O_3/H_2O_2/Fe^{3+}$ (pH 7)	2.03	0.994
H_2O_2 related systems		
UV/H_2O_2 (pH 4)	4.96	0.972
UV/H_2O_2 (pH 7)	4.08	0.985
UV/H_2O_2 (pH 10)	1.99	0.986
UV/H_2O_2/Fe^{3+} (pH 7)	4.59	0.976
O_3 related systems		
UV/O_3 (pH 4)	1.91	0.977
UV/O_3 (pH 7)	2.91	0.975
UV/O_3 (pH 10)	6.59	0.998
UV/O_3/Fe^{3+} (pH 7)	2.90	0.958
H_2O_2/O_3 hybrid related systems		
UV/O_3/H_2O_2 (pH 7)	5.33	0.972
UV/$O_3/H_2O_2/Fe^{3+}$ (pH 7)	5.78	0.976

Note: values in brackets presented the result of 20 ppm RR2.

(i) under alkaline conditions, ozone rapidly decomposes to yield hydroxyl and other radicals in solutions (Eqs. (10)–(12));
(ii) under acidic conditions, ozone remains stable and reacts directly with organic substrates [34].

Since the oxidation potential of hydroxyl radicals markedly exceeds that of ozone molecules, direct oxidation is slower than radical oxidation [14]. Alaton et al. [35] revealed that increasing ozonation system pH increases hydroxyl radical production; restated, the decolorization rate increases as pH increases. Combining ozone with UV light promotes dye degradation via direct and indirect production of hydroxyl radicals following ozone decomposition and hydrogen peroxide formation, respectively (Eqs. (9) and (13)) [36]:

$$O_3 + OH^- \rightarrow O_3^{-}\bullet + OH\bullet \quad (10)$$

$$O_3^{-}\bullet \rightarrow O^{-}\bullet + O_2 \quad (11)$$

$$O^{-}\bullet + H^+ \rightarrow OH\bullet \quad (12)$$

$$O_3 + H_2O + h\nu \rightarrow O_2 + H_2O_2 \quad (13)$$

$$H_2O_2 + h\nu \rightarrow 2OH\bullet \quad (9)$$

The combined process is more effective because UV radiation promotes ozone decomposition, yielding additional hydroxyl radicals, and, thus, increasing ozonation. Various studies have indicated that UV promotes ozone decolorization [1–3,9,36].

Fig. 6 shows the UV–vis spectral changes of RR2 at pH 7 in UV/O_3 systems. Before treatment, the UV–vis spectra of

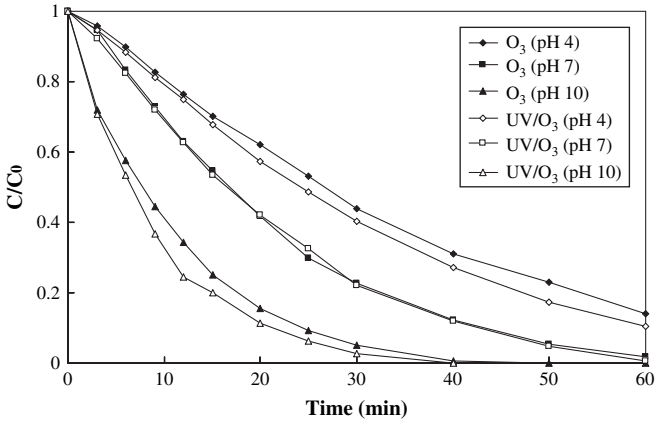

Fig. 5. Effects of pH on the decolorization efficiency in O_3 and UV/O_3 systems (RR2 = 40 ppm, ozone flow rate = 500 mL/min and $T = 25\ ^\circ C$).

RR2 have three main absorption bands − two in the UV region (285 and 330 nm) and one in visible region (538 nm). The UV band is characteristic of two adjacent rings, whereas the visible band is associated with a long conjugated π system linked by two azo groups [37]. The intensity of absorption at 538 nm declined extremely rapidly, from 0.99 to 0.20, after 20 min. The UV bands at 285 nm (from 0.82 to 0.46) and 370 nm (from 0.26 to 0.13) vanished after 20 min and at a slower rate than did the visible band. The hydroxyl radicals initially attack the azo groups and open the N═N bond (Fig. 6); the N═N bonds are more easily destroyed than are aromatic structures. Lucas and Peres [26] obtained a similar result for C.I. Reactive Black 5 in a photo-Fenton system.

The effect of initial dye concentration on decolorization rate was examined by varying the initial concentration of RR2 20 in the O_3 system; Fig. 7 plots the experimental results. The k values achieved for 20 ppm RR2 at pHs 4, 7 and 10 were 1.75, 4.19 and 7.36 h^{-1}, respectively, and those for 40 ppm RR2 were 1.67, 2.91 and 5.74 h^{-1}, respectively. The decolorization rate decreased as dye concentration increased, partially because additional dye molecules and reaction intermediates competed with hydroxyl radicals and ozone molecules when the dye concentration was high. Several studies have reported similar observations for homogeneous and heterogeneous photocatalytic systems [3,38–40].

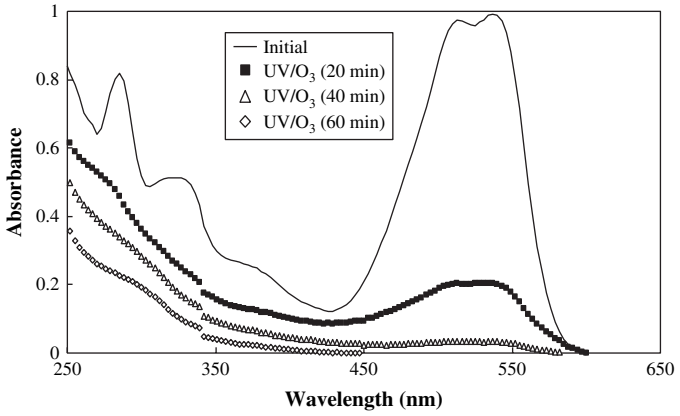

Fig. 6. UV–vis spectral changes of RR2 in UV/O_3 systems (RR2 = 40 ppm, ozone flow rate = 500 mL/min, pH = 7 and $T = 25\ ^\circ C$).

3.4. Decolorization efficiency of the H_2O_2/ozone-related hybrid systems

Fig. 8 presents the decolorization efficiencies of the O_3, O_3/H_2O_2, O_3/Fe^{3+} and $O_3/H_2O_2/Fe^{3+}$ systems at pH 7. The decolorization rate constants for the O_3, O_3/H_2O_2, O_3/Fe^{3+} and $O_3/H_2O_2/Fe^{3+}$ systems at pH 7 followed the order: O_3 (2.91 h^{-1}) > O_3/Fe^{3+} (2.42 h^{-1}) > $O_3/H_2O_2/Fe^{3+}$ (2.03 h^{-1}) > O_3/H_2O_2 (1.42 h^{-1}) (Table 1). This indicates that combining H_2O_2, Fe^{3+} and H_2O_2/Fe^{3+} within the O_3 system at pH 7 did not enhance decolorization. Under acidic conditions, Fe^{2+} catalyzes O_3 decomposition to generate hydroxyl radicals [41]. The O_3/Fe^{3+} system exhibits no such synergic effect. Under alkaline conditions, H_2O_2 can react with O_3, producing hydroxyl and hydroperoxyl radicals (Eq. (14)) [11].

$$O_3 + H_2O_2 \rightarrow O_2 + OH^\bullet + HO_2^\bullet \quad (14)$$

However, as Eq. (14) does not apply under acidic and neutral conditions, adding H_2O_2 to the O_3 system did not increase decolorization. H_2O_2 exhibited negligible decolorization efficiency at pH 7 (Fig. 1) and H_2O_2 scavenged hydroxyl radicals from the solution (Eq. (7)). Hence, combining H_2O_2 with the O_3 system at pH 7 suppressed the decolorization reactions. Esplugas et al. [25] demonstrated that the organic degradation rate of O_3 exceeds that of the O_3/H_2O_2 system.

Fig. 9 shows the decolorization efficiencies obtained for the UV/O_3, UV/H_2O_2, UV/O_3/H_2O_2, UV/O_3/Fe^{3+}, UV/H_2O_2/Fe^{3+} and UV/$O_3/H_2O_2/Fe^{3+}$ systems at pH 7. The decolorization rate constants for the UV/O_3, UV/H_2O_2, UV/O_3/H_2O_2, UV/O_3/Fe^{3+}, UV/H_2O_2/Fe^{3+} and UV/$O_3/H_2O_2/Fe^{3+}$ systems at pH 7 followed the order: UV/$O_3/H_2O_2/Fe^{3+}$ (5.78 h^{-1}) > UV/O_3/H_2O_2 (5.33 h^{-1}) > UV/H_2O_2/Fe^{3+} (4.59 h^{-1}) > UV/H_2O_2 (4.08 h^{-1}) > UV/O_3 (2.91 h^{-1}) ≥ UV/O_3/Fe^{3+} (2.90 h^{-1}) (Table 1). Experimental results revealed that adding Fe^{3+} to UV/H_2O_2 and O_3 to UV/H_2O_2 or UV/H_2O_2/Fe^{3+} enhanced decolorization efficiency. In the UV/O_3/Fe^{3+} system, Fe^{3+} promotes

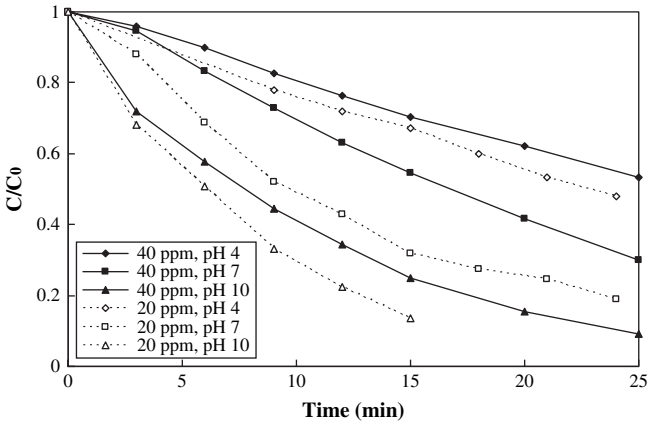

Fig. 7. Effects of dye concentration on the decolorization efficiency in O_3 system at various pHs (RR2 = 40 ppm, ozone flow rate = 500 mL/min and $T = 25\ ^\circ C$).

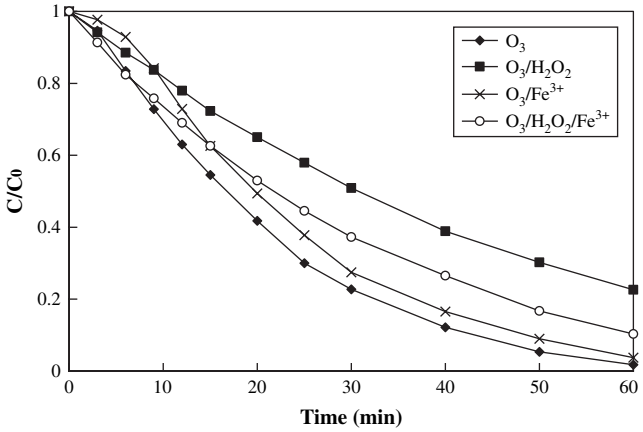

Fig. 8. Decolorization efficiency of O_3, O_3/H_2O_2, O_3/Fe^{3+} and $O_3/H_2O_2/Fe^{3+}$ systems (RR2 = 40 ppm, ozone flow rate = 500 mL/min, H_2O_2 = 1000 ppm, Fe^{3+} = 25 ppm, pH = 7 and T = 25 °C).

formation of hydroxyl radicals (Eq. (1)) and consumes hydroperoxyl radicals (Eq. (6)). The oxidation potential of hydroxyl radicals exceeds that of hydroperoxyl radicals; however, the generation rate of hydroxyl radicals ($3.3 \times 10^{-6}\ M^{-1}\ s^{-1}$) is much lower than the consumption rate of hydroperoxyl radicals ($3.1 \times 10^{5}\ M^{-1}\ s^{-1}$) [17]. Therefore, adding Fe^{3+} did not significantly promote decolorization in the UV/O_3 system.

Eqs. (1)–(9) present the reaction mechanisms in the $UV/H_2O_2/Fe^{3+}$ (photo-Fenton-like) system. Iron cycles between Fe^{3+} and Fe^{2+} under light irradiation. Experimental results indicated that the decolorization rate of the $UV/H_2O_2/Fe^{3+}$ system exceeded that of UV/H_2O_2, which is consistent with findings obtained by previous studies, which showed that the reaction rates of photo-Fenton and photo-Fenton-like systems exceed that of the UV/H_2O_2 system [7,22,27]. In the $UV/O_3/H_2O_2$ system, reactions described by combining Eqs. (9), (13) and (14), which hybrid system had a higher decolorization rate than the UV/O_3, UV/H_2O_2 and O_3/H_2O_2 systems. Interestingly, H_2O_2/Fe^{3+} and O_3/H_2O_2 systems exhibited low decolorization rates; however, the hybrid systems $UV/H_2O_2/Fe^{3+}$ and $UV/O_3/H_2O_2$ had high decolorization rates, implying that UV irradiation played an important role in these systems. Since UV irradiation can decompose H_2O_2 to hydroxyl radicals (Eq. (9)), the scavenging effect of H_2O_2 can be ignored (Eq. (7)), and the decolorization rate is then finally increased. Given the synergic effects in the $UV/H_2O_2/Fe^{3+}$ and $UV/O_3/H_2O_2$ systems, increased decolorization rate in the $UV/O_3/H_2O_2/Fe^{3+}$ system was expected and reasonable. Beltran-Heredia et al. [7] combined O_3 with the $UV/H_2O_2/Fe^{2+}$ system to degrade *p*-hydroxybenzoic acid. Dominguez et al. [22] incorporated O_3 into the $UV/H_2O_2/Fe^{3+}$ system to decolorize Acid Red 2. Both studies suggested that the hybrid O_3/photo-Fenton and O_3/photo-Fenton-like systems had the highest reaction rate among the O_3, O_3/H_2O_2, O_3/Fe^{3+}, O_3/Fe^{2+}, H_2O_2/Fe^{3+}, H_2O_2/Fe^{2+}, $O_3/H_2O_2/Fe^{3+}$, $O_3/H_2O_2/Fe^{2+}$, UV/H_2O_2, $UV/H_2O_2/Fe^{3+}$, $UV/H_2O_2/Fe^{2+}$, UV/O_3, $UV/O_3/Fe^{3+}$, $UV/O_3/Fe^{2+}$ and $UV/O_3/H_2O_2$ systems.

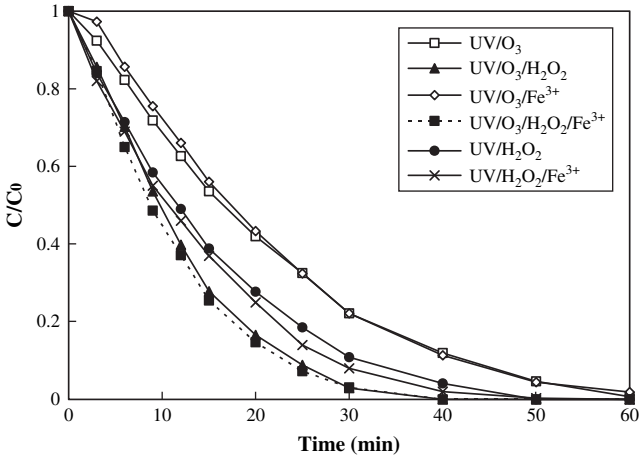

Fig. 9. Decolorization efficiency of UV/O_3, UV/H_2O_2, $UV/O_3/H_2O_2$, $UV/O_3/Fe^{3+}$, $UV/H_2O_2/Fe^{3+}$ and $UV/O_3/H_2O_2/Fe^{3+}$ systems (RR2 = 40 ppm, ozone flow rate = 500 mL/min, H_2O_2 = 1000 ppm, Fe^{3+} = 25 ppm, pH = 7 and T = 25 °C).

4. Conclusions

Neither UV nor H_2O_2 alone caused significant RR2 decolorization. As the H_2O_2 concentration was increased from 500 to 1000 ppm in the UV/H_2O_2 system, decolorization efficiency increased; however, at $H_2O_2 > 1000$ ppm, no further improvement occurred. Attention must be paid to the molar Fe^{3+}:H_2O_2 ratio to prevent undesired radical scavenging reactions. The k values of the UV/H_2O_2 system followed the order of pH 4 > pH 7 > pH 10; the k values for the UV/O_3 system exceeded those obtained for O_3 and the k values of the O_3 and UV/O_3 systems followed the order: pH 10 > pH 7 > pH 4. Without UV irradiation, decolorization rate constants at pH 7 followed the order: $O_3 > O_3/Fe^{3+} > O_3/H_2O_2/Fe^{3+} > O_3/H_2O_2$. Under UV irradiation, the decolorization rate constants at pH 7 followed the order: $UV/O_3/H_2O_2/Fe^{3+} > UV/O_3/H_2O_2 > UV/H_2O_2/Fe^{3+} > UV/H_2O_2 > UV/O_3 \geq UV/O_3/Fe^{3+}$. Notably, UV irradiation was important to the synergic effects of hybrid systems.

Acknowledgements

The authors would like to thank the National Science Council of the Republic of China for financially supporting this research under Contract No. NSC 95-2221-E-212-022.

References

[1] Wu CH, Chang CL, Kuo CY. Decolorization of Amaranth by advanced oxidation processes. Reaction Kinetics and Catalysis Letters 2005;86:37–43.
[2] Wu CH, Chang CL, Kuo CY. Decolorization of Procion Red MX-5B in electrocoagulation (EC), UV/TiO2 and ozone related systems. Dyes and Pigments 2008;76(1):187–94.
[3] Wu CH, Chang CL. Decolorization of Procion Red MX-5B by advanced oxidation processes: comparative studies of the homogeneous and heterogeneous systems. Journal of Hazardous Materials 2006;128:265–72.
[4] Gutowska A, Kaluzna-Czaplinska J, Jozwiak WK. Degradation mechanism of Reactive Orange 113 dye by H_2O_2/Fe^{2+} and ozone in aqueous solution. Dyes and Pigments 2007;74:41–6.

[5] Jozwiak WK, Mitros M, Kaluzna-Czaplinska J, Tosik R. Oxidative decomposition of Acid Brown 159 dye in aqueous solution by H_2O_2/Fe^{2+} and ozone with GC/MS analysis. Dyes and Pigments 2007;74:9–16.
[6] Ghaly MY, Hartel G, Mayer R, Haseneder R. Photochemical oxidation of *p*-chlorophenol by UV/H_2O_2 and photo-Fenton process. A comparative study. Waste Management 2001;21:41–7.
[7] Beltran-Heredia J, Torregrosa J, Dominguez JR, Peres JA. Comparison of the degradation of *p*-hydroxybenzoic acid in aqueous solution by several oxidation processes. Chemosphere 2001;42:351–9.
[8] Kurbus T, Marechal AML, Voncina DB. Comparison of H_2O_2/UV, H_2O_2/O_3 and H_2O_2/Fe^{2+} processes for the decolorisation of vinylsulphone reactive dyes. Dyes and Pigments 2003;58:245–52.
[9] Tezcanli-Guyer G, Ince NH. Individual and combined effects of ultrasound ozone and UV irradiation: a case study with textile dyes. Ultrasonics 2004;42:603–9.
[10] Contreras S, Rodriguez M, Chamarro E, Esplugas S. UV-and UV/Fe(III)-enhanced ozonation in aqueous solution. Journal of Photochemistry and Photobiology A: Chemistry 2001;142:79–83.
[11] Brillas E, Cabot PL, Rodriguez RM, Arias C, Garrido JA, Oliver R. Degradation of the herbicide 2, 4-DP by catalyzed ozonation using the O_3/Fe^{2+}/UVA system. Applied Catalysis B: Environmental 2004;51:117–27.
[12] Konsowa AH. Decolorization of wastewater containing direct dye by ozonation in a bath bubble column reactor. Desalination 2003;158:233–40.
[13] Koch M, Yediler A, Lienert D, Insel G, Kettrup A. Ozonation of hydrolyzed azo dye Reactive Yellow 84 (CI). Chemosphere 2002;46:109–13.
[14] Oguz E, Keskinler B, Celik Z. Ozonation of aqueous Bomaplex Red CR-L dye in a semi-batch reactor. Dyes and Pigments 2005;64:101–8.
[15] Momani FA, Sans C, Esplugas S. A comparative study of the advanced oxidation of 2,4-dichlorophenol. Journal of Hazardous Materials 2004;107:123–9.
[16] Tokumura M, Ohta A, Znad HT, Kawase Y. UV light assisted decolorization of dark brown colored coffee effluent by photo-Fenton reaction. Water Research 2006;40:3775–84.
[17] Kusic H, Koprivanac N, Bozic AL, Selanec I. Photo-assisted Fenton type processes for the degradation of phenol: a kinetic study. Journal of Hazardous Materials 2006;136:632–44.
[18] Alnuaimi MM, Rauf MA, Ashraf SS. Comparative decoloration study of Neutral Red by different oxidative processes. Dyes and Pigments 2007;72:367–71.
[19] Modirshahla N, Behnajady MA, Ghanbary F. Decolorization and mineralization of C.I. Acid Yellow 23 by Fenton and photo-Fenton processes. Dyes and Pigments 2007;73:305–10.
[20] Arslan-Alaton I. Degradation of a commercial textile biocide with advanced oxidation processes and ozone. Journal of Environmental Management 2007;82:145–54.
[21] Kusic H, Koprivanac N, Srsan L. Azo dye degradation using Fenton type processes assisted by UV irradiation: a kinetic study. Journal of Photochemistry and Photobiology A: Chemistry 2006;181:195–202.
[22] Dominguez JR, Beltran J, Rodriguez O. Vis and UV photocatalytic detoxification methods (using TiO_2, TiO_2/H_2O_2, TiO_2/O_3, $TiO_2/S_2O_8^{2-}$, O_3, H_2O_2, $S_2O_8^{2-}$, Fe^{3+}/H_2O_2 and $Fe^{3+}/H_2O_2/C_2O_4^{2-}$) for dyes treatment. Catalysis Today 2005;101:389–95.
[23] Brillas E, Calpe JC, Cabot PL. Degradation of the herbicide 2,4-dichlorophenoxyacetic acid by ozonation catalyzed with Fe^{2+} and UVA light. Applied Catalysis B: Environmental 2003;46:381–91.
[24] Skoumal M, Cabot PL, Centellas F, Arias C, Rodriguez RM, Garrido JA, et al. Mineralization of paracetamol by ozonation catalyzed with Fe^{2+}, Cu^{2+}, and UVA light. Applied Catalysis B: Environmental 2006;66:228–40.
[25] Esplugas S, Gimenez J, Contreras S, Pascual E, Rodriguez M. Comparison of different advanced oxidation processes for phenol degradation. Water Research 2002;36:1034–42.
[26] Lucas S, Peres JA. Decolorization of the azo dye Reactive Black 5 by Fenton and photo-Fenton oxidation. Dyes and Pigments 2006;71:236–44.
[27] Muruganandham M, Swaminathan M. Advanced oxidative decolourisation of Reactive Yellow 14 azo dye by UV/TiO_2, UV/H_2O_2, UV/H_2O_2/Fe^{2+} processes – a comparative study. Separation and Purification Technology 2006;48:297–303.
[28] El-Morsi TM, Emara MM, Bary HMHAE, Abd-El-Aziz AS, Friesen KJ. Homogeneous degradation of 1,2,9,10-tetrachlorodecane in aqueous solutions using hydrogen peroxide, iron and UV light. Chemosphere 2002;47:343–8.
[29] Hoffmann MR, Martin ST, Choi W, Bahnemann DW. Environmental applications of semiconductor photocatalysis. Chemical Reviews 1995;95:69–96.
[30] Pignatello JJ, Liu D, Huston P. Evidence for an additional oxidant in the photoassisted Fenton reaction. Environmental Science and Technology 1999;33:1832–9.
[31] Ruppert G, Bauer R, Heisler G. UV-O_3, UV-H_2O_2, UV-TiO_2 and photo-Fenton – comparison of advanced oxidation processes for wastewater treatment. Chemosphere 1994;28:1447–54.
[32] Tang WZ, Huang P. Stoichiometry of Fenton's reagent in the oxidation of chlorinated aliphatic organic pollutants. Environmental Technology 1997;18:13–23.
[33] Buxton GV, Greenstock CL, Helman WP, Ross AB. Critical review of rate constants for reactions of hydrated electrons, hydrogen atoms and hydroxyl radicals ($OH^{\bullet}/O^{-\bullet}$) in aqueous solution. Journal of Physical and Chemical Reference Data 1988;17:513–886.
[34] Glaze WH, Kang JW, Chapin DH. The chemistry of water treatment processes involving ozone, hydrogen, and ultraviolet radiation. Ozone Science and Engineering 1987;9:335–52.
[35] Alaton IA, Balcioglu IA, Bahnemann DW. Advanced oxidation of a reactive dyebath effluent: comparison of O_3, H_2O_2/UV-C and TiO_2/UV-A processes. Water Research 2002;36:1143–54.
[36] Peyton GR, Glaze WH. The mechanism of photolytic ozonation. Abstract of Papers – American Chemical Society 1985;189:5.
[37] Silverstein RMC, Basdler GC, Morrill GC. Spectrophotometric identification of organic compounds. New York: Wiley; 1991.
[38] So CM, Cheng MY, Yu JC, Wong PK. Degradation of azo dye Procion Red MX-5B by photocatalytic oxidation. Chemosphere 2002;46:905–12.
[39] Neppolian B, Choi HC, Sakthivel S, Arabindoo B, Murugesan V. Solar/UV-induced photocatalytic degradation of three commercial textile dyes. Journal of Hazardous Materials 2002;89:303–17.
[40] Sakthivel S, Neppolian B, Shankar MV, Arabindoo B, Palanichamy M, Murugesan V. Solar photocatalytic degradation of azo dye: comparison of photocatalytic efficiency of ZnO and TiO_2. Solar Energy Materials and Solar Cells 2003;77:65–82.
[41] Sedlack DL, Hoigne F, David MM, Colvile RN, Seyffer E, Acker K, et al. The cloudwater chemistry of iron and copper at Great Dun Fell, U.K. Atmospheric Environment 1997;31:2515–26.